Anaphylatoxin C5a Creates a Favorable Microenvironment for Lung Cancer Progression

Leticia Corrales,* Daniel Ajona,* Stavros Rafail,[†] Juan J. Lasarte,[‡] Jose I. Riezu-Boj,[‡] John D. Lambris,[†] Ana Rouzaut,[*,§] Maria J. Pajares,[*,¶] Luis M. Montuenga,[*,¶] and Ruben Pio[*,§]

The complement system contributes to various immune and inflammatory diseases, including cancer. In this study, we investigated the capacity of lung cancer cells to activate complement and characterized the consequences of complement activation on tumor progression. We focused our study on the production and role of the anaphylatoxin C5a, a potent immune mediator generated after complement activation. We first measured the capacity of lung cancer cell lines to deposit C5 and release C5a. C5 deposition, after incubation with normal human serum, was higher in lung cancer cell lines than in nonmalignant bronchial epithelial cells. Notably, lung malignant cells produced complement C5a even in the absence of serum. We also found a significant increase of C5a in plasma from patients with non-small cell lung cancer, suggesting that the local production of C5a is followed by its systemic diffusion. The contribution of C5a to lung cancer growth in vivo was evaluated in the Lewis lung cancer model. Syngeneic tumors of 3LL cells grew slower in mice treated with an antagonist of the C5a receptor. C5a did not modify 3LL cell proliferation in vitro but induced endothelial cell chemotaxis and blood-vessels formation. C5a also contributed to the immunosuppressive microenvironment required for tumor growth. In particular, blockade of C5a receptor significantly reduced myeloid-derived suppressor cells and immunomodulators ARG1, CTLA-4, IL-6, IL-10, LAG3, and PDL1 (B7H1). In conclusion, lung cancer cells have the capacity to generate C5a, a molecule that creates a favorable tumor microenvironment for lung cancer progression. *The Journal of Immunology*, 2012, 189: 4674–4683.

T he complement system is a central part of the innate immune response. Complement plays a major role as a first defense against microbes and unwanted host molecules (1). Complement also participates in diverse physiological processes and contributes to various immune and inflammatory diseases (2). There are three conventional mechanisms of complement activation, known as the classical, lectin, and alternative pathways. They differ in the initial activation steps and converge in the cleavage of C3, which generates its active fragment C3b. The subsequent steps are the formation of the C5 convertase and the assembly of the membrane attack complex. During complement activation, soluble multifunctional proinflammatory peptide fragments C3a and C5a are released from C3 and C5, respectively. These molecules are referred to as anaphylatoxins and play a variety of biological activities in the immune response (3).

There is increasing evidence for the contribution of complement activation to cancer progression. During carcinogenesis, tumor cells acquire genetic and epigenetic alterations that dictate their malignant growth. Because of these alterations, the complement system can recognize tumor cells, as can be shown by the complement deposition found in different tumors (4–8). However, cancer cells can resist the harmful effects of complement by different extracellular and intracellular mechanisms (9). In fact, new findings on the contribution of complement to tumor growth have challenged the paradigm that complement protects against tumors (10). One of the first pieces of evidence came from a study demonstrating that the generation of anaphylatoxin C5a in the tumor microenvironment leads to significant tumor progression in a mouse model of cervical cancer. This effect seems to be mediated by the recruitment of myeloid-derived suppressor cells (MDSCs) and the generation of an immunosuppressive microenvironment (11). Complement activation may also be linked to angiogenesis. The presence of C5a in drusen of patients with age-related macular degeneration has been associated with the development of chronic neovascularization (12). Nevertheless, the role of C5a in angiogenesis is controversial, and anti-angiogenic effects of this molecule have also been shown in a model of retinopathy of prematurity (13).

In the current study, we evaluated the implication of C5a in lung carcinogenesis. Lung cancer is the leading cause of death among all cancers (14). There are two main histological types of lung cancer: small cell lung cancer and non-small cell lung cancer (NSCLC), the latter accounting for 80–85% of all cases. In human lung cancers, the immune response strongly influences tumor progression

(15). Some observations suggest that complement activation is important in this malignancy. For example, elevated complement levels correlating with tumor size have been found in lung cancer patients (16). However, lung tumor cells resist complement attack by the expression of membrane-bound and soluble complement regulators (17–20). In this context, we hypothesized that complement activation may contribute to the generation of an inflammatory microenvironment that favors lung tumor progression. We found that lung cancer cell lines are able to generate higher levels of C5a than those of nonmalignant lung epithelial cells. We also found a significant increase of C5a in plasma from patients with NSCLC. Using a murine syngeneic lung cancer model, we demonstrate the contribution of C5a to lung cancer growth by the generation of a protumor microenvironment. These results provide novel information about the relationship between complement activation and lung cancer, which may influence the development of future therapeutic strategies.

Materials and Methods

Cell lines and primary cultures

Mouse Lewis lung carcinoma (3LL) and human lung cancer cell lines were obtained from the American Type Culture Collection. Cells were grown in RPMI 1640 supplemented with 2 mM glutamine, 10% Fetalclone (Thermo), 100 U/ml penicillin, and 100 μg/ml streptomycin (Invitrogen). Immortalized normal human bronchial epithelial cells (HBECs) were established by introducing mouse Cdk4 and hTERT into normal HBECs (21, 22). The genetic alterations introduced in these cells are not sufficient to confer a full malignant phenotype. Two HBEC lines from two different donors were used: HBEC3-KT and HBEC10-KT. These cell lines were kindly provided by Dr. J.D. Minna (University of Texas Southwestern Medical Center, Dallas, TX). Cells were maintained in keratinocyte serum-free medium supplemented with human recombinant epidermal growth factor (EGF) and bovine pituitary extract (Life Technologies). The immortalized BEAS-2B cells were obtained from American Type Culture Collection and cultured in DMEM–Ham's F-12 (1:1) supplemented with human recombinant EGF, insulin, transferrin, epinephrine, triiodothyronine, retinoic acid, hydrocortisone, gentamicin sulfate/amphotericin-B, and bovine pituitary extract (Lonza). HUVECs were obtained from Lonza and maintained in EGM2MV–EBM-2 medium supplemented with human recombinant EGF, vascular endothelial growth factor (VEGF), basic fibroblast growth factor (bFGF), long R3 insulin-like growth factor-1, hydrocortisone, ascorbic acid, heparin, gentamicin sulfate/amphotericin-B, and 2% fetal bovine serum (Lonza).

Patients

Plasma samples from 50 patients with advanced lung cancer (adenocarcinomas or squamous cell carcinomas at stages IIIB and IV) and from 50 healthy people (matched by age, sex, and smoking exposure) were obtained from EDTA-treated blood at the Clínica Universidad de Navarra (Pamplona, Spain). The study protocol was approved by the institutional ethical committee, and all patients gave informed consent. Lung tumors were classified according to the World Health Organization 2004 classification (23). C5a concentration was quantified in the plasma samples using the commercial kit Human Complement Component C5a (DuoSet; R&D Systems), following the manufacturer's instructions.

Peptides

The cyclic hexapeptide AcF(OP(D)ChaWR) [acetylated phenylalanine–(ornithine-proline-(D)cyclohexylalanine-tryptophan-arginine)], a C5aR antagonist, was used in in vitro and in vivo experiments to block C5aR activity. The cyclic hexapeptide AcF(OP(D)ChaA(D)R) [acetylated phenylalanine–(ornithine-proline-(D)cyclohexylalanine-alanine-(D)arginine)] was used as control. Both peptides were derived from the C-terminal decapeptide sequence of C5a, which was modified to produce either antagonists or peptides with no activity (7). Both peptides were synthesized by PeptideSynthetics (Fareham, U.K.).

C5 deposition

Cells were detached from culture dishes with trypsin/EDTA, washed, and resuspended in veronal buffer with magnesium (1.8 mM barbital, 3.1 mM barbituric acid, 141 mM NaCl, 0.5 mM $MgCl_2$, pH 7.4). Human NSCLC and immortalized bronchial cells (2×10^5) were incubated with 20% normal human serum (NHS) or heat-inactivated normal human serum (HI-NHS) for 30 min at 37°C. Mouse 3LL cells were incubated with 40% normal mouse serum (NMS) or heat-inactivated normal mouse serum (HI-NMS). In human cells, C5 deposition was assessed using a polyclonal goat anti-human C5b (Quidel) in binding buffer and FITC-conjugated rabbit anti-goat IgG (Serotec). In mouse cells, C5 deposition was assessed using an mAb against mouse-C5 (clone Bb5.1) and Alexa Fluor-conjugated goat anti-mouse IgG (Invitrogen). After the addition of 7-aminoactinomycin D (BD Biosciences), cells were washed and analyzed by flow cytometry in a FACSCalibur with CellQuest software (BD Biosciences). Data were collected as mean fluorescence intensity.

C5a production in serum-free conditions

Cells were cultured for 24 h in 100 mm² plates (2×10^6 cells/10 ml) or 24-well plates (10^5 cells/0.5 ml). Afterward, cells were washed three times with PBS, and 10 or 0.5 ml of RPMI 1640 basal medium was added, respectively. Conditioned media were collected after 48 h. C5a concentration was assessed by ELISA using the commercial kit Human Complement Component C5a (DuoSet; R&D Systems). Local C5a production by A549 cells was also evaluated in the presence of different inhibitors: compstatin, inhibitor of complement C3; antithrombin III (Sigma) plus heparin (Rovi), inhibitor of the coagulation system; lepirudin (Schering AG), inhibitor of thrombin; GM6001 (Millipore), metalloproteinase inhibitor; E-64 (Sigma), cysteine protease inhibitor; and serine protease inhibitors aprotinin (Trasylol; Bayer), soybean trypsin inhibitor (SBTI; Sigma), and TLCK (Sigma). In the case of compstatin, an improved 3-analogue with the sequence D-Tyr-Ile-[Cys-Sar-Val-Asp-Trp-Ala-His-Trp(1-Me)-Gln-Arg-Cys]-N-Me-Ile and a corresponding control peptide D-Tyr-Ile-[Cys-Val-Trp(1-Me)-Gln-Asp-Trp-Sar-Ala-His-Arg-Cys]-N-Me-Ile were synthesized as described (24).

mRNA expression of complement proteins

Total RNA was purified using the RNeasy Kit (Qiagen), following the manufacturer's instructions. Reverse transcription was done using 2 μg of total RNA, SuperScript III (Invitrogen), and random hexamers (Applied Biosystems). Expression of human complement components C1q, C1r, C1s, C2, C4, C3, C5, factor B, factor D, and properdin was assessed by real-time PCR using commercial TaqMan probes (Applied Biosystems). PCR conditions were as follows: 2 min at 50°C, 10 min at 95°C and 40 cycles (15 s at 95°C and 1 min at 60°C). Results were expressed for each gene as the relative gene expression normalized to the IPO8 mRNA expression (25).

Expression of C5aR in HUVECs and 3LL cells was studied by conventional PCR using human GAPDH and mouse HPRT as control genes, respectively. Primers used in conventional PCR are listed in Table I. PCR reactions were performed using 1 μl cDNA, 10 μl 2× Master Mix buffer (Promega), and 500 nM sense and antisense primers (Sigma) in a total volume of 20 μl. For human C5aR and GAPDH, the reactions were performed according to the following conditions: 92°C for 2 min, followed by 30 cycles (30 s at 92°C, 30 s at 51°C, and 30 s at 72°C). For mouse C5aR and HPRT, the following steps were performed: 92°C for 2 min, followed by 35 cycles (1 min at 92°C, 1 min at 61°C, 1 min at 72°C). PCR products were separated on agarose gels and stained with ethidium bromide (Invitrogen).

Syngeneic mouse model of lung cancer

Female C57BL/6J mice of 8–12 wk were used (Harlan Laboratories). The experimental protocols were reviewed and approved by the Institutional Animal Care and Use Committee of the University of Navarra. Murine 3LL cells (2.5×10^4) were resuspended in 100 μl PBS and mixed with 100 μl growth factor-reduced Matrigel (BD Biosciences). Cells were injected s.c. in the right flanks. For the pharmacological blockade of C5aR, mice received an s.c. injection of C5aR antagonist AcF(OP(D)ChaWR) every 3 d at a dose of 1 mg per kilogram body weight in 200 μl PBS, starting 24 h before the inoculation of tumor cells. The control peptide AcF(OP(D)ChaA(D)R) was used with the same administration regimen. For the blockade of C5 activity, mice received i.p. 1 mg of the anti-mouse C5 mAb Bb5.1 or an IgG control isotype in 100 μl PBS every 3 d, starting 4 h before the inoculation of cells. In all cases, tumors were measured every 3 d, and the tumor volumes were calculated by the formula $(L \times W^2)/2$, where L is the length and W is the width.

Expression of C5aR by flow cytometry

C5aR expression on HUVEC and 3LL cells was detected by flow cytometry. Cells (2×10^5) were incubated for 30 min at 4°C with rat anti-mouse C5aR

(20/70; BioLegend) or mouse anti-human C5aR (S5/1; Serotec) in PBS, 1% BSA, 0.1% azide. After two washes, cells were incubated for 30 min at 4°C with the secondary Abs: FITC-conjugated rabbit anti-rat IgG (Serotec) or Alexa Fluor-conjugated goat anti-mouse IgG (Invitrogen). Finally, cells were washed twice and analyzed by flow cytometry on a FACSCalibur using CellQuest Pro software (BD Biosciences). Data were expressed as mean fluorescence intensity.

Cell proliferation

The MTT assay was used to study the proliferation of HUVEC and 3LL cell lines treated with human or murine C5a, respectively. For endothelial cells, 1.5×10^3 HUVECs were seeded in assay medium (EGM-2MV without rhVEGF and rhFGF) in a 96-well plate. After 24 h of incubation, dilutions of human C5a (Calbiochem) from 1 ng/ml to 2 µg/ml were added. Wells without cells were used as background. One hundred percent growth was established using cells grown in assay medium alone. bFGF at 10 ng/ml (Sigma) was used as positive control. All treatments were performed in sextuplicate. After 96 h of incubation, 10 µl of a 5 mg/ml MTT solution (Sigma) was added to each well. Plates were incubated for 4 h at 37°C, and then 100 µl of solubilization buffer (10% SDS, 50% N,N-dimethylformamide, pH 4.7) was added. Plates were left on the cell incubator overnight. One day later, absorbance was measured at 540 nm with a reference wavelength of 690 nm in a Sunrise microplate reader (Tecan). For 3LL cells, 2×10^3 cells were seeded in RPMI 1640 complemented with 0.5% Fetalclone. Next day, dilutions of murine C5a (R&D Systems) from 0.01 to 500 ng/ml were added in basal RPMI. Wells without cells were used as background. One hundred percent growth was assessed in wells with no C5a added. Cells were incubated for 48 h at 37°C. The assay was developed as indicated above.

To measure the percentage of proliferation, the mean value in each condition was calculated by the formula:

$$\text{Proliferation}(\%) = \frac{\text{Absorbance}_{\text{treatment concentration}} - \text{Absorbance}_{\text{background}}}{\text{Absorbance}_{\text{100\% proliferation}} - \text{Absorbance}_{\text{background}}} \times 100.$$

HUVEC migration

For the evaluation of the chemotactic effect of C5a in HUVECs, 7.5×10^4 cells were cultured in 24-well plates in EBM-2 basal medium on the upper chamber of Transwells with 8-µm pore size (Corning-Costar). C5a dilutions ranging from 500 to 0.25 ng/ml were added. EBM-2 medium and EBM-2 medium with 10% fetal bovine serum were used as negative and positive control, respectively. Cells were allowed to migrate for 48 h in a cell culture incubator. Afterward, cells from the upper chambers were removed by swiping with cotton swabs, and cells adhered to the lower side of Transwells were fixed with 4% formaldehyde (Panreac) and stained with 0.5% crystal violet (Sigma). Migrated cells on the lower surface of the filter were visualized and photographed using an inverted microscope (Leyca DM ILM). At least five fields at ×10 magnification were taken and counted using ImageJ software (National Institutes of Health).

HUVEC tube formation

C5a ability to promote angiogenesis in vitro was tested using the tube formation assay. This method is widely used to assess the capacity of a molecule to inhibit or stimulate angiogenesis (26). Before experiments, cells were left in EGM-2MV/EBM-2 basal medium (1:1) for 8 h. Afterward, cells were washed and kept in EBM-2 basal medium overnight. The next day, 48-well plates were coated with 150 µl growth factor-reduced Matrigel (BD Biosciences) and allowed to gel for 2 h at 37°C. Matrigel is a commercial basement membrane matrix derived from the Engelbreth–Holm–Swarm mouse sarcoma (27). Cells (2.5×10^4) in EBM-2 basal medium were seeded on the gel and mixed with C5a at 10 ng/ml final dilution. Cells in EBM-2 medium alone were used as control. At least five repetitions were done per condition. Plates were incubated at 37°C for 5 h. Photographs of five random optical fields in the central area of wells were taken at ×10 magnification with a digital camera coupled to a phase microscope (Leica DM IL LED). Total tube length was calculated using ImageJ software (National Institutes of Health).

In vivo Matrigel plug assay

The effect of C5aR signaling in angiogenesis was determined in vivo by the Matrigel plug assay. Female mice at 10–12 wk of age were s.c. injected with 0.5 ml Matrigel containing 2.5×10^4 3LL cells and 500 ng/ml C5aR antagonist [AcF(OP(D)ChaWR)] or control peptide [AcF(OP(D)ChaA(D) R)]. Peptides were also injected 24 h before and after the inoculation of plugs, and one additional injection was performed 3 d later. Six days after inoculation, 25 mg/ml FITC–dextran (Sigma) in 200 µl PBS was injected

i.v. in the tail vein. Mice were sacrificed 15 min later. The plugs were extracted and fixed in 4% formaldehyde for 24 h. Photographs of areas with vessels were taken using a Zeiss Axiovert confocal microscope.

Analysis of splenocyte subpopulations

Spleens from tumor-bearing mice were mechanically disaggregated in 5 ml PBS using cell strainers with 70-µm pore size (BD Biosciences). Single-cell suspensions ($\sim 5 \times 10^5$ splenocytes) were preincubated with an mAb to mouse CD16-CD32 (Fc block; 2.4G2; BD Pharmingen) and then incubated with a labeled primary Ab against mouse CD4 (RM4-5), CD8a (53-6.7), CD11b (M1/70), or Ly6C/Gr1 (AL-2) (all from BD Biosciences) diluted in FACS buffer (PBS, 0.24 µM EDTA, and 5% Fetalclone). Staining of mouse regulatory T cells was performed using a kit from eBioscience according to the manufacturer's instructions.

Expression of immune molecules within the tumors

Portions of ~ 0.1 cm^3 (a sphere with 0.6-cm diameter) were cut from the edge of tumors, frozen in dry ice, and maintained at $-80°C$ until the extraction procedure. Total RNA was extracted and retrotranscribed to cDNA. Expression of molecules related to the immune response was performed by real-time PCR using specific primers for each gene (Table II) as previously described (28).

Statistical analysis

Significant differences were evaluated using the Student t test, except in the case of the immune cells and molecules, for which the differences in expression were analyzed by the Mann–Whitney U test. Data were analyzed using GraphPad Prism 5 (GradPad Software). The p values <0.05 were considered statistically significant.
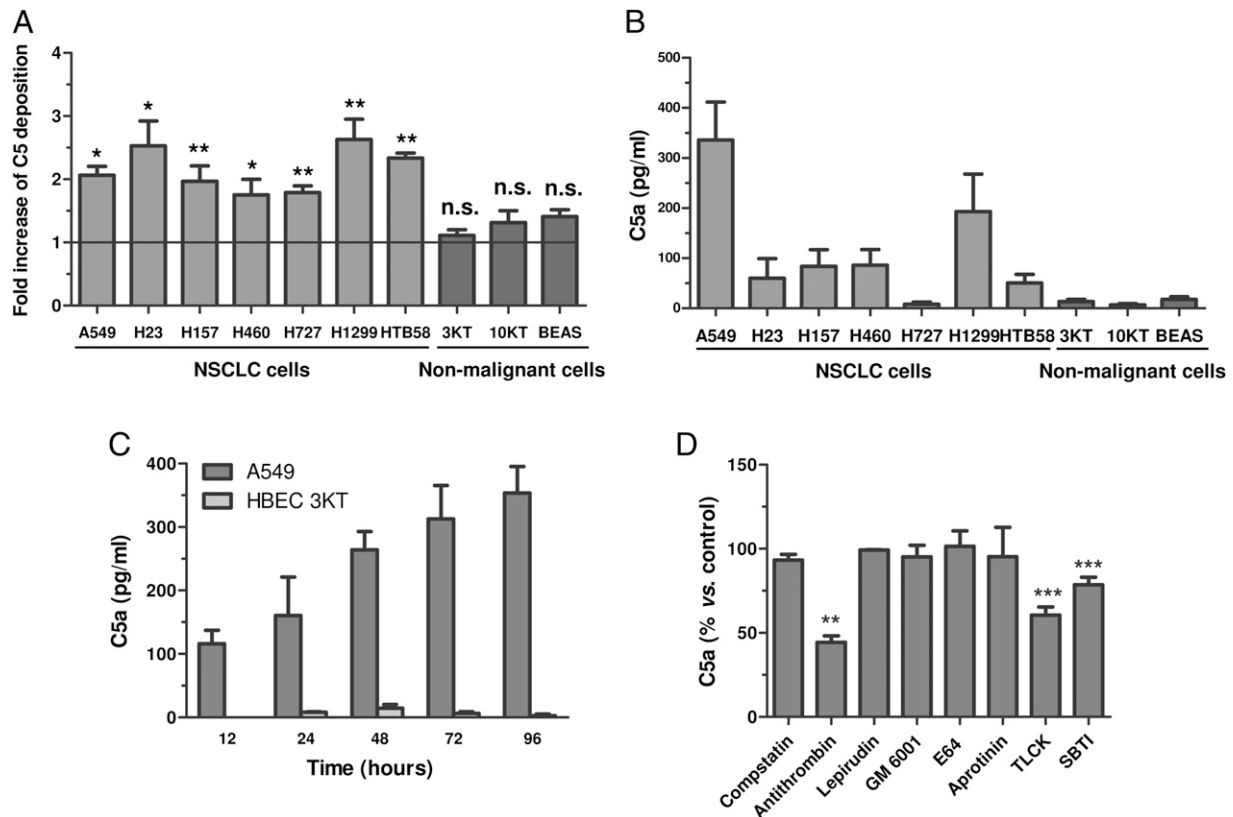
Results

Lung cancer cell lines produce C5a in vitro

The capacity of lung cancer cells to activate complement C5 was evaluated in seven human lung cancer cell lines and three non-fully transformed bronchial epithelial cell lines using NHS as the source of complement components. The amount of cell-derived C5a could not be directly quantified due to the presence of C5a in NHS. Alternatively, C5 deposition on cell membranes was evaluated by flow cytometry. C5 deposition was higher in lung cancer cell lines than in nonmalignant bronchial epithelial cells (Fig. 1A). In fact, all lung cancer cell lines showed a significant increase in C5 deposition after incubation with NHS. However, no significant increase in C5 deposition was observed in the nonmalignant bronchial epithelial cells.

Previous studies have demonstrated that some cell types are able to activate complement and release C5a in the absence of serum (29, 30). Therefore, the next objective was to evaluate the capacity of lung cancer cells to generate C5a in serum-free conditions. Previously, the expression of C5 mRNA in these cells was tested using real-time PCR. All malignant and non-fully transformed pulmonary cell lines expressed C5 mRNA, although the levels were appreciably higher in some lung cancer cell lines (Supplemental Fig. 1). To analyze the production of C5a, lung malignant and nonmalignant cells were cultured in serum-free medium for 48 h. Conditioned media were collected, and C5a levels were determined. All malignant cell lines, except H727, produced detectable C5a levels (Fig. 1B). Conversely, C5a was almost undetectable in nonmalignant bronchial epithelial cells. For A549 and HBEC-3KT cells, a time course was performed from 12 to 96 h (Fig. 1C). In A549, C5a levels gradually increased from the beginning to the end of the experiment. However, in HBEC-3KT cells, the levels of C5a did not increase over time.

The alternative complement pathway has been associated with a local production of C5a in some cell types (29). The contribution of this pathway to the production of C5a by lung cancer cells in the absence of serum was investigated. First, the expression of the main components of the alternative pathway (C3, factor B, factor

FIGURE 1. C5 deposition and local production of C5a by lung cancer and non-fully transformed cells. (**A**) C5 deposition on cells incubated with NHS. Deposition was determined by flow cytometry. Results are shown as mean ± SEM and represent the ratio of the mean fluorescence intensity between 20% NHS and 20% HI-NHS. At least three independent experiments were performed for each cell line. In each cell line, statistical differences between cells incubated with NHS or with HI-NHS were evaluated. A horizontal line at ratio = 1 indicates the baseline. (**B**) Local production of C5a by lung cancer and nonmalignant cells in the absence of serum after 48-h incubation in serum-free medium. C5a levels were determined by ELISA. Data represent mean ± SEM from three independent experiments. (**C**) Time course of the production of C5a by A549 and HBEC-3KT cells. (**D**) Local production of C5a in the presence of protease inhibitors: 10 μM compstatin, 0.2 μM antithrombin III (with 10 U/ml heparin), 0.2 μM lepirudin, 25 μM GM6001, 10 μM E-64, 10 U/ml aprotinin, 100 μM TLCK, or 100 μM SBTI. C5a levels in basal medium were set as 100%. In the case of compstatin, 100% C5a production was set in cells incubated with a compstatin control peptide. Results are expressed as mean ± SEM from at least three independent experiments. *$p < 0.05$, **$p < 0.01$, ***$p < 0.001$.

D, and properdin) was examined by real-time PCR (Supplemental Fig. 2). No apparent association was observed between the expression of these complement components and the levels of locally produced C5a. In fact, the expression of properdin was undetectable in most of the cell lines, and factor B was not expressed by any lung cancer cell line, except H727, which was precisely the lung cancer cell line that did not produce C5a. Next, the potential contribution of the classical complement pathway was assessed. Expression of the main classical complement factors (C1q, C1r, C1s, C2, and C4) was analyzed by real-time PCR. No relation was observed between these elements of the classical pathway and the local production of C5a. In particular, C1q expression was not found in any of the cell lines analyzed (Supplemental Fig. 3). To exclude definitively the contribution of C3 convertases, the production of C5a was evaluated in the presence of compstatin, a molecule that prevents the activation of C3 by C3 convertases (31). No decrease in C5a levels was observed using compstatin up to 10 μM (Fig. 1D). C5a can be generated in a complement-independent manner by different proteases (32). Under serum-free conditions, the production of C5a by A549 cells was significantly reduced in the presence of antithrombin III and heparin (Fig. 1D). The effect of other protease inhibitors was also studied (Fig. 1D). The production of C5a was not affected by the presence of the thrombin inhibitor lepirudin, the metalloproteinase inhibitor GM6001, the cysteine protease inhibitor E64, or the serine protease inhibitor aprotinin. However, SBTI and TLCK,

inhibitors of trypsin-like serine proteases, significantly reduced the local production of C5a. At the concentrations used, these inhibitors did not affect cell proliferation, as determined by MTT assays (data not shown).

Anaphylatoxin C5a levels are increased in plasma of NSCLC patients

Generation of C5a by tumor cells may be followed by its systemic diffusion. Therefore, it can be speculated that C5a can be detected in peripheral blood from lung cancer patients. The concentration of C5a in plasma from 50 patients diagnosed with NSCLC was determined and compared with the concentration of this protein in 50 samples from control individuals matched by age, sex, and smoking exposure (Fig. 2). Cancer patients showed significantly higher C5a plasma levels than control donors (27.76 ± 11.53 versus 14.08 ± 8.24 ng/ml; $p < 0.001$). No statistical differences were found between adenocarcinomas and squamous cell carcinomas or between stage IIIB and IV (data not shown).

Blockade of C5aR slows tumor growth in vivo

The influence of C5a on lung tumor progression in vivo was studied using a syngeneic mouse model of lung cancer. In this model, 3LL cells were injected s.c. in the right flank of C57BL/6J mice. C5a activity was blocked by the administration of the cyclic hexapeptide AcF(OP(D)ChaWR), a C5aR antagonist. Prior to the use of this in vivo model, the capacity of 3LL cells to deposit C5 when
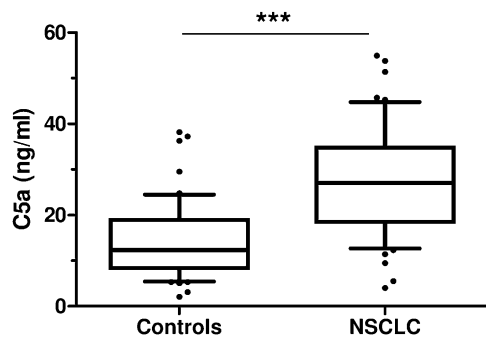
**FIGURE 2.** Quantification of C5a in plasma samples from control donors and patients with NSCLC. ***$p < 0.001$.

incubated with mouse serum in vitro was confirmed (Fig. 3A). Then, 3LL cells were injected in the right flank of mice treated with the C5aR antagonist or with the control cyclic hexapeptide AcF(OP(D) ChaA(D)R). Blockade of C5aR significantly decreased tumor growth (Fig. 3B). To support this result further, treatment with an anti-C5 mAb (Bb5.1) also slowed down tumor growth, although in this case the results did not reach statistical significance (Supplemental Fig. 4). Finally, the addition of C5a to 3LL cells did not modify their in vitro proliferation (Fig. 3C), suggesting that the in vivo effect of C5a on tumor growth is mediated by other mechanisms.

C5a promotes angiogenesis

To elucidate the mechanisms by which C5a/C5aR supports tumor growth in vivo, the role of C5a in angiogenesis was studied. First, the effect of C5a in HUVEC proliferation and migration was evaluated. The expression of C5aR in HUVECs, both at the mRNA and protein levels, was verified (Fig. 4A, 4B, Table I). Proliferation assays were performed in HUVECs cultured for 96 h in the presence of a wide range of C5a concentrations. No effect of C5a on HUVEC proliferation was observed (Fig. 4C). The capacity of C5a to induce HUVEC migration was investigated using the Transwell chamber assay. HUVECs were plated on Transwells and cultured during 48 h with different concentrations of C5a. This factor induced HUVEC chemotaxis with a typical bell-shaped dose-response curve (Fig. 4D). A significant increase in migration, compared with the untreated cells, was observed within 0.125 and 5 ng/ml of C5a ($p_{0.125} = 0.015$; $p_{0.25} < 0.001$; $p_{0.5} = 0.012$; $p_5 < 0.001$). The effect of C5a on the formation of tube-like structures on Matrigel was also tested. HUVECs were plated on gelled Matrigel in EBM-2 medium. After 5 h of incubation, HUVECs treated with 10 ng/ml C5a showed more numerous tube-like structures than cells in basal medium ($p = 0.001$) (Fig. 4E, 4F).

A Matrigel plug assay was performed to evaluate the effect of C5a on angiogenesis in vivo. Matrigel plugs mixed with 3LL cells and the C5aR antagonist or the control peptide were injected in the flanks of C57BL/6J mice. Peptides were injected throughout the experiment as explained in *Materials and Methods*. Six days after inoculation, FITC-conjugated dextran was injected i.v., and animals were sacrificed within 10–15 min. Mice treated with the C5aR antagonist showed less microvessels within their plugs than those treated with the control peptide (Fig. 5A).

In explanted tumors from the 3LL syngeneic mouse, the expression of the angiogenic factors VEGF and bFGF was analyzed (Fig. 5B). There were no differences in VEGF mRNA levels. However, there was a significantly lower expression of bFGF mRNA in tumor extracts from animals treated with the C5aR antagonist ($p = 0.023$). However, there were no differences in tumor vascular density (CD31 staining) between mice treated with
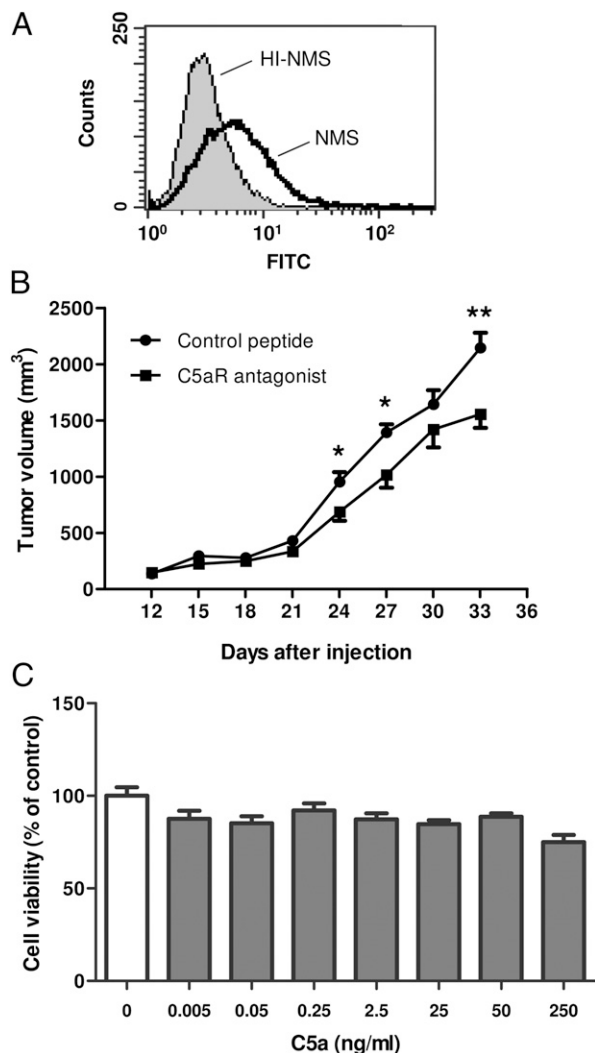

FIGURE 3. Effect of C5aR blockade on 3LL growth. (**A**) C5 deposition in 3LL cells, measured by flow cytometry, after incubation of the cells with 40% NMS (white peak) or HI-NMS (shaded peak). (**B**) Tumor growth of 3LL cells injected s.c. in mice treated with a C5aR antagonist or a control peptide (10 mice per group). Tumor volume is expressed as mean ± SEM. Data are representative of two independent experiments. (**C**) MTT assay with 3LL cells incubated for 48 h in medium with C5a at different concentrations. The graph shows one representative experiment of three independent repetitions. Results show the percentage of viability compared with cells grown in the absence of C5a. Data are expressed as mean ± SEM. *$p < 0.05$, **$p < 0.01$.

the C5a antagonist and those treated with the control peptide (data not shown). In tumors from animals treated with the anti-C5 Bb5.1 mAb, a reduction in the expression of bFGF mRNA, close to statistical significance, was observed ($p = 0.089$; Supplemental Fig. 4).

C5aR blockade reduces immunosuppression

C5a has been proved to be a key factor in the immune regulation of tumors, mainly by the recruitment of MDSCs (11). The effect of C5aR blockade in the immune response to the lung tumors was assessed. For that purpose, splenocyte subpopulations in 3LL tumor-bearing mice treated with the C5aR antagonist or the control peptide were analyzed. There were no differences in the percentages of CD4$^+$, CD8$^+$, and regulatory T cells; however, total MDSCs were significantly reduced when C5aR was blocked ($p = 0.028$; Fig. 6). Both monocytic and granulocytic MDSCs were reduced, although the differences were statistically signifi-
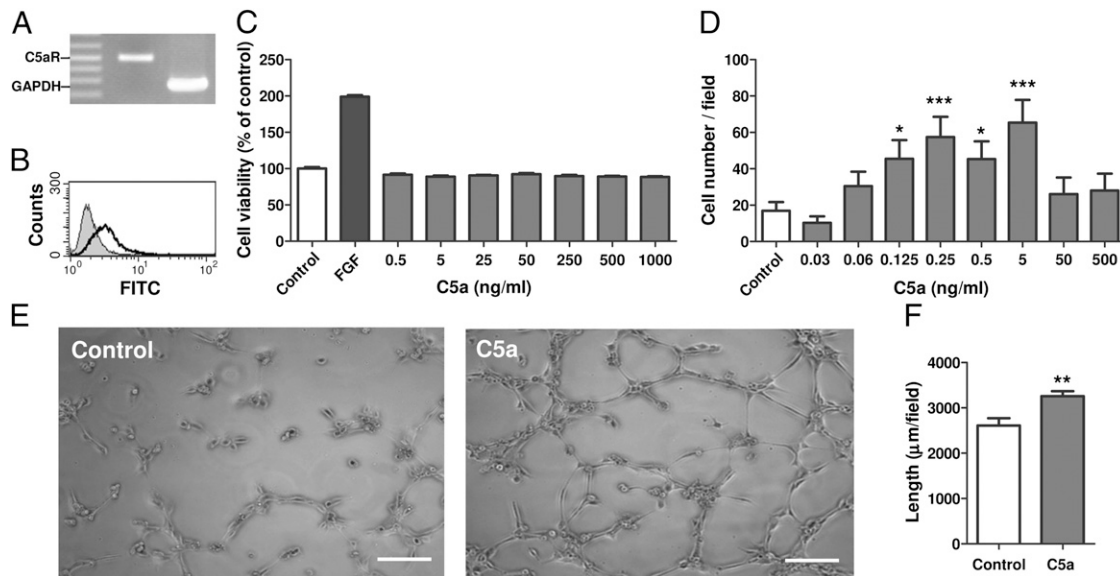
FIGURE 4. Effect of C5a on HUVECs. (**A**) C5aR mRNA expression in HUVECs as determined by PCR (Table I). Detection of GAPDH mRNA was used as positive control. (**B**) C5aR expression on HUVECs assessed by flow cytometry. Cells were incubated with (white peak) or without (shaded peak) an anti-C5aR Ab. (**C**) Proliferation assay with cells incubated with C5a at different concentrations in basal medium for 96 h. Negative and positive controls were performed with basal medium or with 10 ng/ml bFGF, respectively. One representative experiment is shown. Results are expressed as mean $\pm$ SEM and represent the percentage of viability compared with untreated cells. (**D**) Effect of C5a on HUVEC migration in the Transwell assay. C5a was added at different concentrations in basal medium on the lower side of the Transwells. HUVECs were plated in the upper chambers. After 48 h, cells that had migrated to the underside of the Transwells were fixed and stained with crystal violet. Cell migration in each Transwell was analyzed by counting cells in eight different fields. Data are collected from three independent experiments and show mean $\pm$ SEM. $*p < 0.05$, $***p < 0.001$. (**E**) Effect of C5a on the formation of tube-like structures by HUVECs. Cells were plated on gelled Matrigel, and C5a was added at 10 ng/ml. After 5 h, photographs were taken. Representative pictures of tube-like structures taken at original magnification $\times 10$ are shown. Scale bars, 100 μm. (**F**) Quantification of the tube-like structures was performed examining five high-power fields per well using a $\times 10$ objective. The total length of each picture was measured using ImageJ software (National Institutes of Health). Mean $\pm$ SEM is shown. Results are representative of three independent experiments, each one with at least five wells per condition. $**p < 0.01$.

cant only in the subpopulation of granulocytic MDSCs ($p = 0.095$ and $p = 0.015$, respectively). These results suggest that C5a is able to induce an immunosuppressive microenvironment that can be reversed when the C5a receptor is blocked. To confirm this observation, an evaluation of the expression of several immune-related molecules in the tumor microenvironment was carried out. Total RNA was extracted from explanted tumors of animals treated with the C5aR antagonist or the control peptide. Real-time PCR was performed for 22 molecules (Table II). Some of them could not be detected (IL-2, IL-4, FOXP3, IFN-γ, IL-12p35, and OX40L), and others did not show any change between the two treatment groups; namely, IDO, TNF-α, PD1, CCL17, CCL22, GITR, TGF-β, MCP1, granzyme A, granzyme B, and perforin (data not shown). However, the expression of ARG1, CTLA-4, IL-6, IL-10, LAG3, and PDL1 was significantly decreased in tumors from animals treated with the C5aR antagonist (Fig. 7). Most of these molecules are commonly associated with an immunosuppressive state. Blockade of C5 with the Bb5.1 mAb confirmed the downregulation of some immune molecules within the tumors (Supplemental Fig. 4). These results confirm that C5a is implicated in the generation of an immunosuppressive tumor microenvironment.

Discussion

In this study, we provide evidence for the contribution of C5a to the generation of a tumor microenvironment that favors lung cancer progression. Three major observations support this conclusion: i) Lung cancer cell lines are able to generate C5a; ii) the levels of this anaphylatoxin are increased in plasma of NSCLC patients; and iii) the blockade of C5aR in a murine syngeneic lung cancer model slows tumor growth and reduces angiogenesis and the immunosuppressive tumor microenvironment.

Lung carcinogenesis is a multistep process in which normal cells acquire genetic and epigenetic alterations that result in the expression of many cancer-associated molecules. Our results suggest that this neoplastic transformation is accompanied by an increase in the capacity of malignant cells to activate complement. In particular, we found that lung cancer cell lines are able to deposit C5 and generate C5a more efficiently than nonmalignant cells. The generation of C5a within tumors, followed by its systemic diffusion, may explain the increase of C5a found in the plasma of patients with NSCLC. Surprisingly, the ability of tumor cells to produce C5a was increased even in the absence of an exogenous source of complement components (i.e., serum). This capacity had previously been demonstrated in bone marrow cells (30), APCs,

Table I. Sequences of primers used in conventional PCR

Gene	Sense (5′ to 3′)	Antisense (5′ to 3′)
Human C5aR	TGCTGACCATACCCTCCTTC	CCCTAACCACGGACTCTTCA
Human GAPDH	ACTTTGTCAAGCTCATTTCC	CACAGGGTACTTTATTGATG
Mouse C5aR	TACCACAGAACCCAGGAGGA	GCAGGAGGAAGGTGTAGCAG
Mouse HPRT	TGACACTGGCAAAACAATGCA	GGTCCTTTTCACCAGCAAGCT
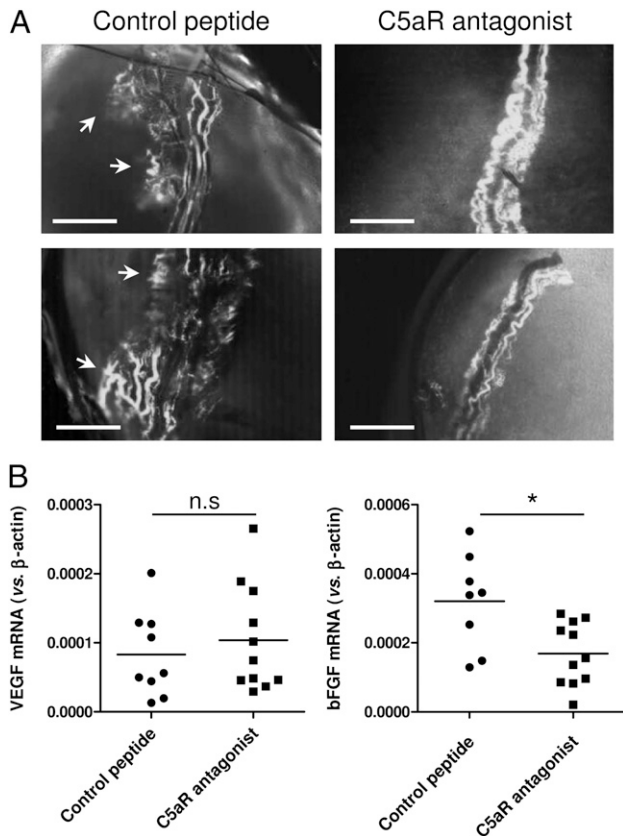
FIGURE 5. Effect of C5a on angiogenesis. (**A**) Matrigel plugs containing 3LL and 500 ng/ml of the C5aR antagonist or the control peptide were implanted s.c. in the flanks of C57BL mice. Peptides were also injected s.c. (at 1 mg/kg of body weight) 24 h before and after implantation of plugs. Six days later, FITC-labeled dextran was injected i.v., and plugs were extracted and fixed. Visualization of vessels was performed in a Zeiss Axiovert confocal microscope at original magnification ×2.5. Representative photographs of each group are shown. Arrows in the control images point to new vessels formed from the preexisting vasculature. Scale bars, 1 mm. (**B**) Expression of angiogenic factors in 3LL tumors. Total mRNA was extracted from tumors of mice treated with the control peptide or the C5aR antagonist. mRNA levels of VEGF and bFGF were determined by real-time PCR and expressed as relative to the β-actin mRNA in each tumor. Individual results per animal and mean per group are shown. *$p < 0.05$.

and T cells (29). In these cases, cells produce functional C3, factor B, and factor D and, as a consequence, are able to activate the alternative pathway of complement. However, in lung cancer cell lines, the implication of the alternative pathway is unlikely, due to the absence of any connection between the expression of complement factors and the local production of C5a. In addition, our results seem to rule out the implication of the classical pathway and, more generally, the implication of any activation pathway in which the C3 convertases are involved. On the basis of these observations, we conclude that C5a is generated by an extrinsic complement activation mechanism. Several bypass routes have been shown to trigger complement immune response (33, 34). Anaphylatoxins can be generated by the action of soluble and membrane-bound proteases, such as serine proteases of the co-agulation and fibrinolysis systems or cell-bound proteases in phagocytic cells (31, 35–37). Our results show that antithrombin III is able to inhibit the production of C5a under serum-free conditions, suggesting that thrombin would be a potential prote-ase able to cleave C5 produced by lung cancer cells. However, lepirudin, a direct thrombin inhibitor, did not affect C5a produc-
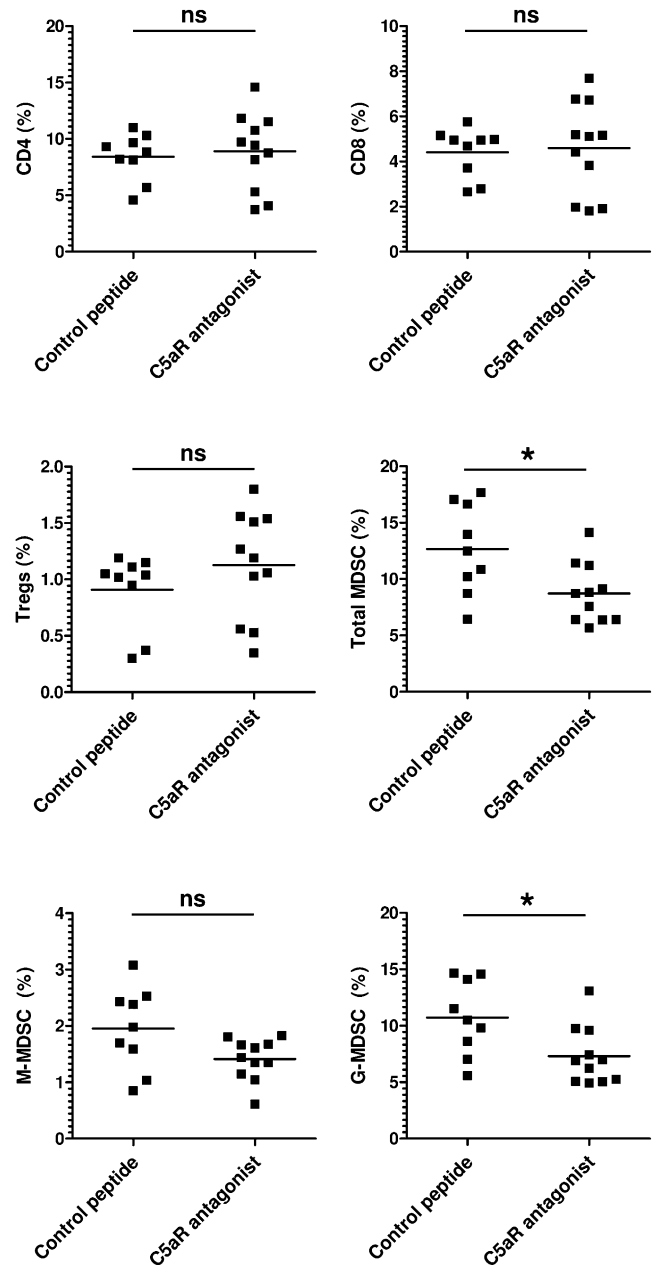
FIGURE 6. Effect of C5aR blockade on splenocyte subpopulations. Graphs represent data from flow cytometry analyses of splenocytes obtained from 3LL tumor-bearing mice injected subcutaneously with the control peptide or the C5aR antagonist at a dose of 1 mg/kg of body weight. Splenocytes were stained with specific Abs to CD4^{+}, CD8^{+}, CD4^{+}CD25^{+}Foxp3^{+} (Treg), and CD11b^{+}Ly6c^{+} (MDSC). Within the MDSC population, subpopulations of monocytic (M-MDSC) and granulocytic (G-MDSC) MDSCs, with high and low expression of Ly6c, respectively, were also analyzed. Individual results per animal and mean per group are shown. *$p < 0.05$.

tion. Apart from thrombin, antithrombin can also inactivate other proteases involved in blood coagulation, as well as serine pro-teases that are not involved in the coagulation cascade such as trypsin (38). It has also been shown that trypsin is able to cleave C5 into biologically active C5a-like fragments (39). In our study, TLCK and SBTI inhibited the production of C5a by A549 cells. TLCK is a serine protease inhibitor with trypsin-like specificity (40). SBTI inhibits different proteases, including trypsin. Con-sidering that A549 cells secrete trypsin-like proteins (41), it can be suggested that C5a can be generated independently of the estab-

Table II.   Sequences of primers used in real-time PCR

| Gene	Sense (5' to 3')	Antisense (5' to 3')
IDO	CCTTGAAGACCACCACATAG	AGCACCTTTCGAACATCGTC
TNF-α	CTTCCAGAACTCCAGGCGGT	GGTTTGCTCGACGTGGGC
IL-2	TGTTGATGGACCTACAGGAG	GTGTTGTCAGAGCCCTTTAG
IL-4	GCTATTGATGGGTCTCAACC	TCTGTGGTGTTCTTCGTTGC
FOXP3	GTTTCTCAAGCACTGCCAAG	TGTGGAAGAACTCTGGGAAG
PD1	ACTGGTCGGAGGATCTTATG	ATCTTGTTGAGGTCTCCAGG
CCL17	TGAGGTCACTTCAGATGCTG	GGACAGTCAGAAACACGATG
CCL22	TCATTAGACACCTGACGAGG	CTTCCACATTGGCACCATAG
GITR	GGAGTCTCAAGGGGATATTG	GGAACTGGAAGCTGCAAGC
TGF-β	CGGCAGCTGTACATTGAC	TCAGCTGCACTTGCAGGAGC
IFN-γ	TCAAGTGGCATAGATGTGGAAGAA	TGGCTCTGCAGGATTTTCATG
MCP1	ACCAGCCAACTCTCACACTGAAGC	CAGAATTGCTTGAGGTGGTTGTG
Granzyme A	AAGGAGCCAGAACAACAG	TAGGTAGGTGAAGGATAGCC
Granzyme B	CAAAGAACAGGAGAAGACCC	AGCCACATAGCACACATC
Perforin	AATAACGACTGGCGTGTG	AGATGAGCCTGTGGTAAG
ARG1	TGGGGAAAGCCAATGAAGAG	AGGAGAAAGGACACAGGTTG
CTLA-4	TCATGTACCCACCGCCATAC	TAGACCCCTGTTGTAAGAGG
IL-6	ACAAAGCCAGAGTCCTTCAG	TGGATGGTCTTGGTCCTTAG
IL-10	GGACAACATACTGCTAACCG	AATCACTCTTCACCTGCTCC
IL-12p35	CACGCTACCTCCTCTTTTTG	AGGCAACTCTCGTTCTTGTG
LAG3	CTCTTTGGAGGCAGAAATCG	CTCTTTGGAGGCAGAAATCG
PDL1	GATCATCCCAGAACTGCCTG	GCTTACGTCTCCTCGAATTG
OX40L	AGTGGAAGAAGACGCTAAGG	TCCTCACATCTGGTAACTGC
β-Actin	CGCGTCCACCCGCGAG	CCTGGTGCCTAGGGCG

lished pathways by the action of a trypsin-like protease produced by lung tumor cells. Some trypsin-like serine proteases, such as plasmin and urokinase plasminogen activator, have been reported to be involved in tumor progression and metastasis (42, 43). Therefore, we speculate that the blockade of this yet unknown protease may inhibit the capacity of tumor cells to produce C5a, reducing its tumor promoting effects.

Tumor promoting activities of complement C5a may be associated with induction of angiogenesis and generation of an immunosuppressive microenvironment. In fact, angiogenesis and immunosuppression may occur simultaneously in response to diverse physiological stimuli (44). Previous reports support the proangiogenic activity of C5a. The activation of C5aR in endothelial cells causes cell retraction, increased paracellular permeability, and eosinophil transmigration (45). It has also been demonstrated that C5a induces genes that promote the effects of VEGF (46). The effect of C5a in endothelial cell proliferation and migration has also been proposed (47–49). In our experimental conditions, C5a enhanced cell migration and formation of tube-like structures in a gelled matrix, although we observed no effect of C5a on HUVEC cell proliferation. These results strongly suggest that C5a has angiogenic properties in vitro; however, the role of C5a in angiogenesis in vivo is still controversial. Some studies support the proangiogenic potential of C5a, whereas others sustain the contrary. An anti-angiogenic effect of C3 and C5 has been demonstrated in a model of retinopathy of prematurity, where C5a stimulated macrophages toward an angiogenesis-inhibitory phenotype (13). On the contrary, the proangiogenic role of C3a and C5a has been demonstrated in age-related macular degeneration and in animals submitted to laser-induced choroidal neovascularization (12). Taking together, these results suggest that the effect of C5a on angiogenesis is influenced by physiological and timing variables. Consequently, the activity of C5a in cancer may be affected by the time of analysis. In a mouse model of cervical cancer, no differences in vascular permeability were observed when animals were treated with the C5aR peptide antagonist (11). Similarly, in our lung cancer model, there were no differences in tumor vascular density at the end of the experiment. Still, the

expression of bFGF, a potent mitogen and chemotactic factor for endothelial cells (50), was significantly reduced within the tumors of the animals treated with the C5aR antagonist. Besides, the C5aR antagonist had an inhibitory effect in the formation of vessels in Matrigel plugs of 3LL cells after 6-d incubation, suggesting that C5a may be important in the promotion of angiogenesis in the early steps of tumor formation.

The immunosuppressive capacity of complement C5a has also been addressed in this work. The pharmacological blockade of C5aR diminished the population of MDSCs in the spleen of tumor-bearing mice. MDSCs are a heterogeneous population of myeloid progenitor cells and immature myeloid cells with an immunosuppressive function in tumor immunity (51). This result is in full agreement with previous observations. The MDSC population is increased in the spleen of tumor-bearing mice and in blood of patients with cancer (52). Markiewski et al. (11) found that in a cervical cancer model, the generation of C5a in the tumor microenvironment enhanced tumor growth by the recruitment of MDSCs and the suppression of the antitumor T cell-mediated response. In the current study, we characterized the expression of immune-related molecules in the tumor microenvironment generated by the inhibition of C5aR. The blockade of C5a signaling downregulated the expression of key immunosuppressive molecules within the tumors. These molecules included ARG1, IL-10, IL-6, CTLA-4, LAG3, and PDL1. Most of these immune regulators are mediators of regulatory T cell activity (53). Besides, many of them have been associated with the development of lung cancer (54), and some of them have been found elevated in blood of patients with NSCLC (55–57). Using the 3LL lung carcinoma model, Rodriguez et al. (58) reported a production of ARG1 by myeloid cells in the tumor microenvironment, which impaired T cell function and favored tumor growth. IL-10 transgenic mice injected with 3LL cells developed larger tumors than control mice, suggesting that the production of IL-10 prevents the development of an effective immune response against the tumor cells (59). IL-6 is a pleiotropic cytokine that may have proinflammatory or anti-inflammatory effects. In the tumor microenvironment, IL-6 promotes immunosuppression through the induction of immunosup-
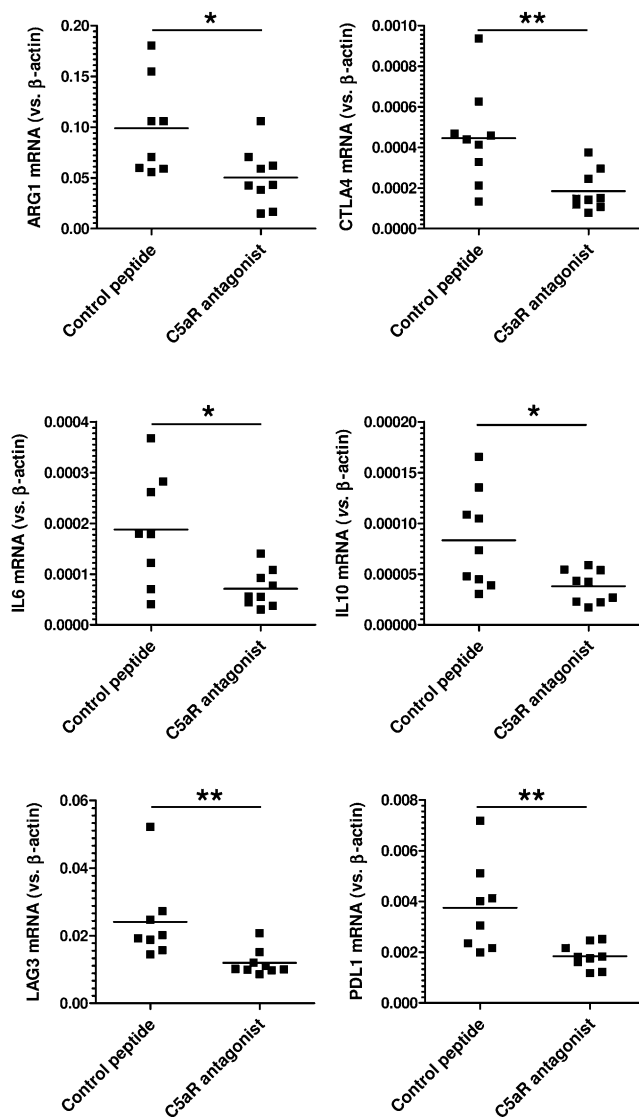
FIGURE 7. mRNA expression in 3LL tumors of molecules related to the immune response. Total mRNA was extracted from tumors of mice treated with the control peptide or the C5aR antagonist. mRNA levels were determined by real-time PCR and expressed as relative to the β-actin mRNA in each tumor. Individual results per animal and mean per group are shown. $*p < 0.05$, $**p < 0.01$.

pressive molecules, such as B7-H4 (60). CTLA-4 inhibits T cell activation when it binds to CD80 and CD86 on APCs (61). CTLA-4 and LAG3 have immunosuppressive functions associated with their expression by regulatory T cells (62, 63). Finally, PDL1 (B7-H1) is overexpressed in various human tumors, including lung cancer, and contributes to negative regulation in anti-tumor immune responses (64, 65). Remarkably, Ab-mediated blockage of PDL1–PD1 interaction induced durable responses in patients with advanced cancer, including NSCLC, a tumor type traditionally considered not to be responsive to immunotherapy (66, 67).

In conclusion, our results further support the role of complement activation in cancer progression. In particular, we demonstrate that lung cancer cell lines substantially activate complement and release C5a. Subsequently, this complement mediator orchestrates fundamental biological processes that promote angiogenesis and immunosuppression. These results support the rationale of blockade of complement factors to increase the efficacy of future therapeutic strategies.

References

1. Walport, M. J. 2001. Complement. First of two parts. *N. Engl. J. Med.* 344: 1058–1066.
2. Ricklin, D., G. Hajishengallis, K. Yang, and J. D. Lambris. 2010. Complement: a key system for immune surveillance and homeostasis. *Nat. Immunol.* 11: 785–797.
3. Klos, A., A. J. Tenner, K. O. Johswich, R. R. Ager, E. S. Reis, and J. Köhl. 2009. The role of the anaphylatoxins in health and disease. *Mol. Immunol.* 46: 2753–2766.
4. Bjørge, L., J. Hakulinen, O. K. Vintermyr, H. Jarva, T. S. Jensen, O. E. Iversen, and S. Meri. 2005. Ascitic complement system in ovarian cancer. *Br. J. Cancer* 92: 895–905.
5. Niculescu, F., H. G. Rus, M. Retegan, and R. Vlaicu. 1992. Persistent complement activation on tumor cells in breast cancer. *Am. J. Pathol.* 140: 1039–1043.
6. Niehans, G. A., D. L. Cherwitz, N. A. Staley, D. J. Knapp, and A. P. Dalmasso. 1996. Human carcinomas variably express the complement inhibitory proteins CD46 (membrane cofactor protein), CD55 (decay-accelerating factor), and CD59 (protectin). *Am. J. Pathol.* 149: 129–142.
7. Finch, A. M., A. K. Wong, N. J. Paczkowski, S. K. Wadi, D. J. Craik, D. P. Fairlie, and S. M. Taylor. 1999. Low-molecular-weight peptidic and cyclic antagonists of the receptor for the complement factor C5a. *J. Med. Chem.* 42: 1965–1974.
8. Yamakawa, M., K. Yamada, T. Tsuge, H. Ohrui, T. Ogata, M. Dobashi, and Y. Imai. 1994. Protection of thyroid cancer cells by complement-regulatory factors. *Cancer* 73: 2808–2817.
9. Jurianz, K., S. Ziegler, H. Garcia-Schüler, S. Kraus, O. Bohana-Kashtan, Z. Fishelson, and M. Kirschfink. 1999. Complement resistance of tumor cells: basal and induced mechanisms. *Mol. Immunol.* 36: 929–939.
10. Rutkowski, M. J., M. E. Sughrue, A. J. Kane, S. A. Mills, and A. T. Parsa. 2010. Cancer and the complement cascade. *Mol. Cancer Res.* 8: 1453–1465.
11. Markiewski, M. M., R. A. DeAngelis, F. Benencia, S. K. Ricklin-Lichtsteiner, A. Koutoulaki, C. Gerard, G. Coukos, and J. D. Lambris. 2008. Modulation of the antitumor immune response by complement. *Nat. Immunol.* 9: 1225–1235.
12. Nozaki, M., B. J. Raisler, E. Sakurai, J. V. Sarma, S. R. Barnum, J. D. Lambris, Y. Chen, K. Zhang, B. K. Ambati, J. Z. Baffi, and J. Ambati. 2006. Drusen complement components C3a and C5a promote choroidal neovascularization. *Proc. Natl. Acad. Sci. USA* 103: 2328–2333.
13. Langer, H. F., K. J. Chung, V. V. Orlova, E. Y. Choi, S. Kaul, M. J. Kruhlak, M. Alatsatianos, R. A. Deangelis, P. A. Roche, P. Magotti, et al. 2010. Complement-mediated inhibition of neovascularization reveals a point of convergence between innate immunity and angiogenesis. *Blood* 116: 4395–4403.
14. Kohler, B. A., E. Ward, B. J. McCarthy, M. J. Schymura, L. A. Ries, C. Eheman, A. Jemal, R. N. Anderson, U. A. Ajani, and B. K. Edwards. 2011. Annual report to the nation on the status of cancer, 1975-2007, featuring tumors of the brain and other nervous system. *J. Natl. Cancer Inst.* 103: 714–736.
15. Sautès-Fridman, C., J. Cherfils-Vicini, D. Damotte, S. Fisson, W. H. Fridman, I. Cremer, and M. C. Dieu-Nosjean. 2011. Tumor microenvironment is multifaceted. *Cancer Metastasis Rev.* 30: 13–25.
16. Nishioka, K., K. Kawamura, T. Hirayama, T. Kawashima, and K. Shimada. 1976. The complement system in tumor immunity: significance of elevated levels of complement in tumor bearing hosts. *Ann. N. Y. Acad. Sci.* 276: 303–315.
17. Varsano, S., L. Rashkovsky, H. Shapiro, D. Ophir, and T. Mark-Bentankur. 1998. Human lung cancer cell lines express cell membrane complement inhibitory proteins and are extremely resistant to complement-mediated lysis; a comparison with normal human respiratory epithelium in vitro, and an insight into mechanism(s) of resistance. *Clin. Exp. Immunol.* 113: 173–182.
18. Ajona, D., Z. Castaño, M. Garayoa, E. Zudaire, M. J. Pajares, A. Martinez, F. Cuttitta, L. M. Montuenga, and R. Pio. 2004. Expression of complement factor H by lung cancer cells: effects on the activation of the alternative pathway of complement. *Cancer Res.* 64: 6310–6318.
19. Ajona, D., Y. F. Hsu, L. Corrales, L. M. Montuenga, and R. Pio. 2007. Downregulation of human complement factor H sensitizes non-small cell lung cancer cells to complement attack and reduces in vivo tumor growth. *J. Immunol.* 178: 5991–5998.
20. Okroj, M., Y. F. Hsu, D. Ajona, R. Pio, and A. M. Blom. 2008. Non-small cell lung cancer cells produce a functional set of complement factor I and its soluble cofactors. *Mol. Immunol.* 45: 169–179.
21. Ramirez, R. D., S. Sheridan, L. Girard, M. Sato, Y. Kim, J. Pollack, M. Peyton, Y. Zou, J. M. Kurie, J. M. Dimaio, et al. 2004. Immortalization of human bronchial epithelial cells in the absence of viral oncoproteins. *Cancer Res.* 64: 9027–9034.
22. Sato, M., M. B. Vaughan, L. Girard, M. Peyton, W. Lee, D. S. Shames, R. D. Ramirez, N. Sunaga, A. F. Gazdar, J. W. Shay, and J. D. Minna. 2006. Multiple oncogenic changes (K-RAS(V12), p53 knockdown, mutant EGFRs, p16 bypass, telomerase) are not sufficient to confer a full malignant phenotype on human bronchial epithelial cells. *Cancer Res.* 66: 2116–2128.

23. Travis, W. D., E. Brambilla, H. K. Müller-Hermelink, and C. C. Harris. 2004. *Pathology and Genetics of Tumours of the Lung, Pleura, Thymus and Heart.* IARC Press, Lyon, France.

24. Qu, H., D. Ricklin, H. Bai, H. Chen, E. S. Reis, M. Maciejewski, A. Tzekou, R. A. Deangelis, R. R. Resuello, F. Lupu, et al. 2012. New analogs of the clinical complement inhibitor compstatin with subnanomolar affinity and enhanced pharmacokinetic properties. *Immunobiology.* In press.

25. Nguewa, P. A., J. Agorreta, D. Blanco, M. D. Lozano, J. Gomez-Roman, B. A. Sanchez, I. Valles, M. J. Pajares, R. Pio, M. J. Rodriguez, et al. 2008. Identification of importin 8 (IPO8) as the most accurate reference gene for the clinicopathological analysis of lung specimens. *BMC Mol. Biol.* 9: 103.

26. Ponce, M. L. 2001. *Methods in Molecular Medicine.* Humana Press, Totowa, NJ.

27. Kubota, Y., H. K. Kleinman, G. R. Martin, and T. J. Lawley. 1988. Role of laminin and basement membrane in the morphological differentiation of human endothelial cells into capillary-like structures. *J. Cell Biol.* 107: 1589–1598.

28. Larrea, E., R. Aldabe, E. Molano, C. M. Fernandez-Rodriguez, A. Ametzazurra, M. P. Civeira, and J. Prieto. 2006. Altered expression and activation of signal transducers and activators of transcription (STATs) in hepatitis C virus infection: in vivo and in vitro studies. *Gut* 55: 1188–1196.

29. Strainic, M. G., J. Liu, D. Huang, F. An, P. N. Lalli, N. Muqim, V. S. Shapiro, G. R. Dubyak, P. S. Heeger, and M. E. Medof. 2008. Locally produced complement fragments C5a and C3a provide both costimulatory and survival signals to naive CD4+ T cells. *Immunity* 28: 425–435.

30. Tu, Z., H. Bu, J. E. Dennis, and F. Lin. 2010. Efficient osteoclast differentiation requires local complement activation. *Blood* 116: 4456–4463.

31. Ricklin, D., and J. D. Lambris. 2008. Compstatin: a complement inhibitor on its way to clinical application. *Adv. Exp. Med. Biol.* 632: 273–292.

32. Huber-Lang, M., J. V. Sarma, F. S. Zetoune, D. Rittirsch, T. A. Neff, S. R. McGuire, J. D. Lambris, R. L. Warner, M. A. Flierl, L. M. Hoesel, et al. 2006. Generation of C5a in the absence of C3: a new complement activation pathway. *Nat. Med.* 12: 682–687.

33. Selander, B., U. Mårtensson, A. Weintraub, E. Holmström, M. Matsushita, S. Thiel, J. C. Jensenius, L. Truedsson, and A. G. Sjöholm. 2006. Mannan-binding lectin activates C3 and the alternative complement pathway without involvement of C2. *J. Clin. Invest.* 116: 1425–1434.

34. Zhang, M., K. Takahashi, E. M. Alicot, T. Vorup-Jensen, B. Kessler, S. Thiel, J. C. Jensenius, R. A. Ezekowitz, F. D. Moore, and M. C. Carroll. 2006. Activation of the lectin pathway by natural IgM in a model of ischemia/reperfusion injury. *J. Immunol.* 177: 4727–4734.

35. Amara, U., D. Rittirsch, M. Flierl, U. Bruckner, A. Klos, F. Gebhard, J. D. Lambris, and M. Huber-Lang. 2008. Interaction between the coagulation and complement system. *Adv. Exp. Med. Biol.* 632: 71–79.

36. Markiewski, M. M., B. Nilsson, K. N. Ekdahl, T. E. Mollnes, and J. D. Lambris. 2007. Complement and coagulation: strangers or partners in crime? *Trends Immunol.* 28: 184–192.

37. Huber-Lang, M., E. M. Younkin, J. V. Sarma, N. Riedemann, S. R. McGuire, K. T. Lu, R. Kunkel, J. G. Younger, F. S. Zetoune, and P. A. Ward. 2002. Generation of C5a by phagocytic cells. *Am. J. Pathol.* 161: 1849–1859.

38. Wong, R. F., T. L. Chang, and R. D. Feinman. 1982. Reaction of antithrombin with proteases. Nature of the reaction with trypsin. *Biochemistry* 21: 6–12.

39. Wetsel, R. A., and W. P. Kolb. 1983. Expression of C5a-like biological activities by the fifth component of human complement (C5) upon limited digestion with noncomplement enzymes without release of polypeptide fragments. *J. Exp. Med.* 157: 2029–2048.

40. Rawlings, N. D., F. R. Morton, C. Y. Kok, J. Kong, and A. J. Barrett. 2008. MEROPS: the peptidase database. *Nucleic Acids Res.* 36(Database issue): D320–D325.

41. Miyata, S., N. Koshikawa, S. Higashi, Y. Miyagi, Y. Nagashima, S. Yanoma, Y. Kato, H. Yasumitsu, and K. Miyazaki. 1999. Expression of trypsin in human cancer cell lines and cancer tissues and its tight binding to soluble form of Alzheimer amyloid precursor protein in culture. *J. Biochem.* 125: 1067–1076.

42. Cox, G., W. P. Steward, and K. J. O'Byrne. 1999. The plasmin cascade and matrix metalloproteinases in non-small cell lung cancer. *Thorax* 54: 169–179.

43. Henneke, I., S. Greschus, R. Savai, M. Korfei, P. Markart, P. Mahavadi, R. T. Schermuly, J. Wygrecka, J. Stürzebecher, W. Seeger, et al. 2010. Inhibition of urokinase activity reduces primary tumor growth and metastasis formation in a murine lung carcinoma model. *Am. J. Respir. Crit. Care Med.* 181: 611–619.

44. Motz, G. T., and G. Coukos. 2011. The parallel lives of angiogenesis and immunosuppression: cancer and other tales. *Nat. Rev. Immunol.* 11: 702–711.

45. Jagels, M. A., P. J. Daffern, and T. E. Hugli. 2000. C3a and C5a enhance granulocyte adhesion to endothelial and epithelial cell monolayers: epithelial and endothelial priming is required for C3a-induced eosinophil adhesion. *Immunopharmacology* 46: 209–222.

46. Albrecht, E. A., A. M. Chinnaiyan, S. Varambally, C. Kumar-Sinha, T. R. Barrette, J. V. Sarma, and P. A. Ward. 2004. C5a-induced gene expression in human umbilical vein endothelial cells. *Am. J. Pathol.* 164: 849–859.

47. Langeggen, H., E. Johnson, and G. Hetland. 2001. Effects of C5a and FMLP on interleukin-8 production and proliferation of human umbilical vein endothelial cells. *Inflammation* 25: 83–89.

48. Kurihara, R., K. Yamaoka, N. Sawamukai, S. Shimajiri, K. Oshita, S. Yukawa, M. Tokunaga, S. Iwata, K. Saito, K. Chiba, and Y. Tanaka. 2010. C5a promotes migration, proliferation, and vessel formation in endothelial cells. *Inflamm. Res.* 59: 659–666.

49. Schraufstatter, I. U., K. Trieu, L. Sikora, P. Sriramarao, and R. DiScipio. 2002. Complement c3a and c5a induce different signal transduction cascades in endothelial cells. *J. Immunol.* 169: 2102–2110.

50. Cross, M. J., and L. Claesson-Welsh. 2001. FGF and VEGF function in angiogenesis: signalling pathways, biological responses and therapeutic inhibition. *Trends Pharmacol. Sci.* 22: 201–207.

51. Ostrand-Rosenberg, S., and P. Sinha. 2009. Myeloid-derived suppressor cells: linking inflammation and cancer. *J. Immunol.* 182: 4499–4506.

52. Gabrilovich, D. I., and S. Nagaraj. 2009. Myeloid-derived suppressor cells as regulators of the immune system. *Nat. Rev. Immunol.* 9: 162–174.

53. Cao, X. 2010. Regulatory T cells and immune tolerance to tumors. *Immunol. Res.* 46: 79–93.

54. Montuenga, L. M., and R. Pio. 2007. Tumour-associated macrophages in non-small cell lung cancer: the role of interleukin-10. *Eur. Respir. J.* 30: 608–610.

55. De Vita, F., M. Orditura, G. Galizia, C. Romano, A. Roscigno, E. Lieto, and G. Catalano. 2000. Serum interleukin-10 levels as a prognostic factor in advanced non-small cell lung cancer patients. *Chest* 117: 365–373.

56. Brichory, F. M., D. E. Misek, A. M. Yim, M. C. Krause, T. J. Giordano, D. G. Beer, and S. M. Hanash. 2001. An immune response manifested by the common occurrence of annexins I and II autoantibodies and high circulating levels of IL-6 in lung cancer. *Proc. Natl. Acad. Sci. USA* 98: 9824–9829.

57. Pine, S. R., L. E. Mechanic, L. Enewold, A. K. Chaturvedi, H. A. Katki, Y. L. Zheng, E. D. Bowman, E. A. Engels, N. E. Caporaso, and C. C. Harris. 2011. Increased levels of circulating interleukin 6, interleukin 8, C-reactive protein, and risk of lung cancer. *J. Natl. Cancer Inst.* 103: 1112–1122.

58. Rodriguez, P. C., D. G. Quiceno, J. Zabaleta, B. Ortiz, A. H. Zea, M. B. Piazuelo, A. Delgado, P. Correa, J. Brayer, E. M. Sotomayor, et al. 2004. Arginase I production in the tumor microenvironment by mature myeloid cells inhibits T-cell receptor expression and antigen-specific T-cell responses. *Cancer Res.* 64: 5839–5849.

59. Hagenbaugh, A., S. Sharma, S. M. Dubinett, S. H. Wei, R. Aranda, H. Cheroutre, D. J. Fowell, S. Binder, B. Tsao, R. M. Locksley, et al. 1997. Altered immune responses in interleukin 10 transgenic mice. *J. Exp. Med.* 185: 2101–2110.

60. Kryczek, I., L. Zou, P. Rodriguez, G. Zhu, S. Wei, P. Mottram, M. Brumlik, P. Cheng, T. Curiel, L. Myers, et al. 2006. B7-H4 expression identifies a novel suppressive macrophage population in human ovarian carcinoma. *J. Exp. Med.* 203: 871–881.

61. Scalapino, K. J., and D. I. Daikh. 2008. CTLA-4: a key regulatory point in the control of autoimmune disease. *Immunol. Rev.* 223: 143–155.

62. Read, S., V. Malmström, and F. Powrie. 2000. Cytotoxic T lymphocyte-associated antigen 4 plays an essential role in the function of CD25(+)CD4(+) regulatory cells that control intestinal inflammation. *J. Exp. Med.* 192: 295–302.

63. Huang, C. T., C. J. Workman, D. Flies, X. Pan, A. L. Marson, G. Zhou, E. L. Hipkiss, S. Ravi, J. Kowalski, H. I. Levitsky, et al. 2004. Role of LAG-3 in regulatory T cells. *Immunity* 21: 503–513.

64. Dong, H., S. E. Strome, D. R. Salomao, H. Tamura, F. Hirano, D. B. Flies, P. C. Roche, J. Lu, G. Zhu, K. Tamada, et al. 2002. Tumor-associated B7-H1 promotes T-cell apoptosis: a potential mechanism of immune evasion. *Nat. Med.* 8: 793–800.

65. Konishi, J., K. Yamazaki, M. Azuma, I. Kinoshita, H. Dosaka-Akita, and M. Nishimura. 2004. B7-H1 expression on non-small cell lung cancer cells and its relationship with tumor-infiltrating lymphocytes and their PD-1 expression. *Clin. Cancer Res.* 10: 5094–5100.

66. Brahmer, J. R., S. S. Tykodi, L. Q. Chow, W. J. Hwu, S. L. Topalian, P. Hwu, C. G. Drake, L. H. Camacho, J. Kauh, K. Odunsi, et al. 2012. Safety and activity of anti-PD-L1 antibody in patients with advanced cancer. *N. Engl. J. Med.* 366: 2455–2465.

67. Topalian, S. L., F. S. Hodi, J. R. Brahmer, S. N. Gettinger, D. C. Smith, D. F. McDermott, J. D. Powderly, R. D. Carvajal, J. A. Sosman, M. B. Atkins, et al. 2012. Safety, activity, and immune correlates of anti-PD-1 antibody in cancer. *N. Engl. J. Med.* 366: 2443–2454.